

# Planar Transition Structures in the Epoxidation of Alkenes. A DFT Study on the Reaction of Peroxyformic Acid with Norbornene Derivatives

Mauro Freccero,<sup>†</sup> Remo Gandolfi,<sup>†</sup> Mirko Sarzi-Amadè,<sup>\*,†</sup> and Augusto Rastelli<sup>‡</sup>

Dipartimento di Chimica Organica, Università di Pavia, V.le Taramelli 10, 27100 Pavia, Italy, and  
Dipartimento di Chimica, Università di Modena, Via Campi 183, 41100 Modena, Italy

nmr@chifis.unipv.it

Received July 4, 2002

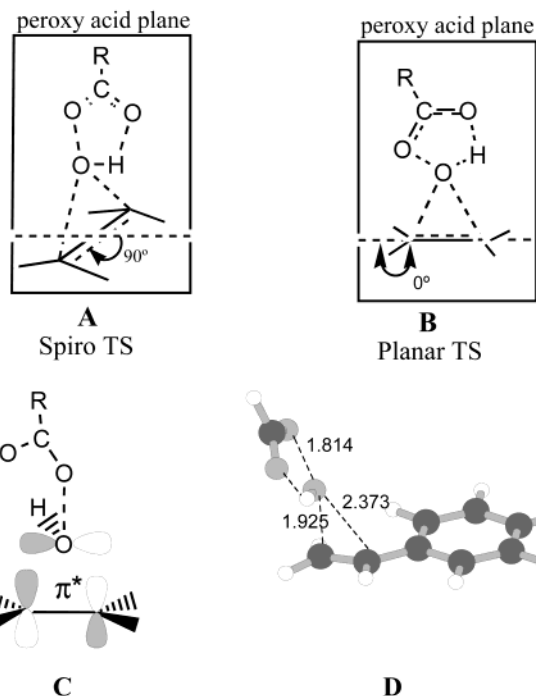
We studied, with the RB3LYP/6-311+G(d,p) method, the mechanism of peroxyformic acid epoxidation of norbornene, norbornadiene, tetramethylethene, and *anti*- and *syn*-sesquinorbornenes. The transition structures (TSs) for the reaction of tetramethylethene and norbornene show a perfect spiro geometry (the peroxy acid plane is perpendicular to the C=C bond axis) with synchronous bond formation. Also three out of the four TSs of the norbornadiene reaction are spiro-like, but the highly asynchronous *syn,endo*-TS has a planar-like geometry. *anti*- and *syn*-sesquinorbornenes are substrates that, because of steric constraints, cannot easily accommodate spiro-like TSs. In fact, we managed to locate only a planar-like TS and a planar TS (the peroxy acid plane contains the C=C bond axis), respectively, for these substrates. These planar TSs are “nonconcerted” since they are strongly unsymmetrical and only one of the C–O bonds of the oxirane ring is significantly formed. IRC analysis, while confirming that formation of one C–O bond fully precedes that of the other, also suggests that all this can take place without formation of intermediates, that is, within a “nonconcerted one-step process”. Our theoretical data correctly reproduce the experimental facial *syn* selectivity of norbornene and norbornadiene epoxidations and compare well with the experimental activation free energies of the peroxy acid epoxidation of all the olefins reported here. This accord validates the method used as adequate to deal with the reactivity of these systems.

## Introduction

The peroxy acid epoxidation of olefins is certainly one of the most useful reactions to synthesize oxirane rings.<sup>1</sup>

Recent good-level DFT calculations, in particular by Bach,<sup>2</sup> Houk,<sup>3</sup> and our group,<sup>4</sup> have firmly established the geometry of transition structures (TSs) for alkene epoxidation with peroxy acids, thus definitely refining the famous “butterfly” transition structure advanced by Bartlett 50 years ago.<sup>5</sup> Computational data indicate that TSs with “spiro” geometry [A (Scheme 1); the peroxy acid plane is perpendicular to the C=C bond axis] are favored

## SCHEME 1



\* To whom correspondence should be addressed. Phone: +39 382 507668. Fax: +39 382 507323.

<sup>†</sup> Università di Pavia.

<sup>‡</sup> Università di Modena.

(1) Schwesinger, J. W.; Bauer, T. Diastereoselective Epoxidation. In *Stereoselective Synthesis*; Helmchen, G., Hoffmann, R. W., Mulzer, J., Schaumann, E., Eds.; Houben Weyl, Thieme: Stuttgart, New York 1995; Vol. E21e, p 4599.

(2) (a) Bach, R. D.; Glukhovtsev, M. N.; Gonzales, C. *J. Am. Chem. Soc.* **1998**, *120*, 9902. (b) Adam, W.; Bach, R. D.; Dmitrenko, O.; Saha-Moller, C. R. *J. Org. Chem.* **2000**, *65*, 6715. (c) Bach, R. D.; Glukhovtsev, M. N.; Gonzales, C.; Marquez, M.; Estevez, C. M.; Baboul, A. G.; Schlegel, H. B. *J. Phys. Chem. A* **1997**, *101*, 6092.

(3) (a) Houk, K. N.; Liu, J.; DeMello, N. C.; Condroski, K. R. *J. Am. Chem. Soc.* **1997**, *119*, 10147. (b) Houk, K. N.; Washington, I. *Angew. Chem., Int. Ed.* **2001**, *40*, 2001.

(4) (a) Freccero, M.; Gandolfi, R.; Sarzi-Amadè M.; Rastelli, A. *J. Org. Chem.* **1999**, *64*, 2030. (b) Freccero, M.; Gandolfi, R.; Sarzi-Amadè M.; Rastelli, A. *J. Org. Chem.* **2000**, *65*, 8948. (c) B3LYP/6-31G\* data: energy (hartrees) –574.510076; dipole moment (D) 4.0855.

(5) Bartlett, P. D. *Rec. Chem. Prog.* **1950**, *47*.

over their “planar” counterparts B (Scheme 1) in which the planar peroxy acid and the C=C bond axis lie in the

same plane. For example, the transition structures of the reaction of peroxyformic acid (PFA) with symmetrically substituted alkenes (e.g., ethene and *cis*-2-butene)<sup>2a</sup> exhibit an exact spiro geometry with synchronous formation of the new C–O bonds of the oxirane ring.

The choice of the spiro arrangement is certainly the result of the intrinsically higher stability of the tetrahedral-like array of atoms around the transferred oxygen in the spiro TS compared to the square-planar-like geometry present in the planar TS. Stabilizing back-donation (from peroxy acid to the CC double bond), involving a p lone pair of the peroxy acid and the  $\pi^*$  of the carbon–carbon double bond (C in Scheme 1), is at its maximum for a perpendicular orientation of the peroxy acid plane to the C=C bond axis, thus favoring the spiro geometry.

It is important to stress that also all the other transition structures reported to date for the reactions of peroxy acids with unsymmetrically substituted double bonds, not only of simple alkenes (propene, isobutene)<sup>2,3a</sup> but also of allylic alcohols (propenol, 2-cyclohexen-1-ol, etc.)<sup>4a,b</sup> and conjugated double bonds (butadiene,<sup>2a,3a</sup> styrene,<sup>4c</sup> and acrylonitrile),<sup>2a,3a</sup> can be classified more or less strictly as spiro TSs<sup>6</sup> since the deviation from perpendicular orientation is always less than 30°. These transition structures continue to be concerted but show some asynchrony in C–O bond formation that can be induced by steric effects, hydrogen-bonding interactions, substituent capability of stabilizing partial charges, etc.

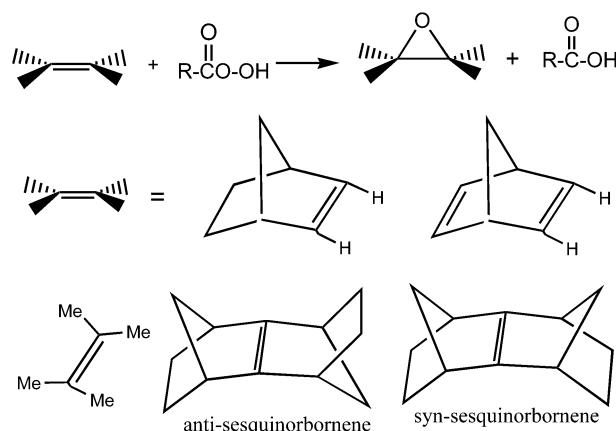
*Asynchrony in bond formation is often accompanied by significant deviation from the ideal spiro geometry.* For example, the transition structure of the PFA epoxidation of styrene (D, Scheme 1), which features a considerable difference in forming the C–O bond length ( $\Delta = 0.45$  Å), exhibits a deviation of 20°. <sup>4c,7</sup>

Less common are asynchronous TSs with ideal spiro geometry. An example is provided by the transition structure for the PFA epoxidation of isobutene in which an almost exact perpendicular orientation of the peroxy acid plane to the C=C bond axis withstands a relevant forming bond asynchrony [ $\Delta = 0.19$  and 0.25 Å at B3LYP/6-31G(d) and B3LYP/6-311+G(d,p), respectively].<sup>2a</sup>

(6) (a) This observation seems to hold rigorously for all closed-shell TSs. When this paper was ready for submission, we became aware of a study (Okovytyy, S.; Gorb, L.; Leszczynski, J. *Tetrahedron Lett.* **2002**, *43*, 4215) on peroxyformic acid epoxidation of ethene at the CASSCF level that indicates a highly unsymmetrical TS with strong diradical character and planar geometry. The authors did not report IRC analysis; thus, it is not quite clear whether this TS leads directly to epoxide or produces an intermediate radical pair ( $\text{HCOO}\cdot + \text{HOCH}_2\text{CH}_2\cdot$ ). An intermediate of this kind for substituted alkenes can lose stereochemistry in contrast with experimental data. Moreover, surprisingly, the authors did not discuss the results of previous CASSCF studies (with a different active space) that indicated a quite symmetrical TS for PFA epoxidation of ethene.<sup>2c</sup> (b) A “nonconcerted” (only one C–O bond is appreciably formed) planar TS with high dipolar character, which leads to the final epoxide without formation of intermediates, was advanced several years ago for the peroxy acid epoxidation of styrene derivatives on the basis of secondary deuterium isotope effects (Hanzlik, R. P.; Shearer, G. O. *J. Am. Chem. Soc.* **1975**, *97*, 5231). At variance with this suggestion our B3LYP calculations indicate that the transition structure of these reactions, although asynchronous, is concerted with spiro-like geometry (see TS D).

(7) Structure D also illustrates the general observation that the peroxy acid plane rotation, away from perpendicular orientation, brings the O–H bond closer to the longer incipient bond. Notice how the peroxy acid plane in TS D is also tilted away from the substituent as a result of a formal rotation around the O–H bond axis. This feature is also evident in the TSs located by Bach et al. for butadiene and acrylonitrile epoxidation reactions.<sup>2a</sup>

## SCHEME 2



As for the energetics, deviation from spiro geometry, through a formal rotation around the peroxy acid breaking O–O bond, should be relatively easy as suggested by the fact that the frequency of the corresponding vibration is always very low, amounting to less than  $<100\text{ cm}^{-1}$ .

The above observations raise the following questions: (i) Can TSs, for peroxy acid epoxidation of alkenes, adopt a planar or planar-like geometry, without a dramatic energy increase, when it is required, for example, by stringent geometrical constraints? (ii) Are planar TSs characterized by a large asynchrony in bond formation with the possibility that the process becomes nonconcerted?

Very appealing models, to computationally answer these questions, are represented by *anti*- and *syn*-sesquinorbornenes (Scheme 2). The epoxidation of these substrates with MCPBA has experimentally been studied by Bartlett et al.<sup>8</sup> and, very recently, by Brown et al.<sup>9a</sup> The latter authors tentatively suggested a planar-like TS in the epoxidation of *anti*-sesquinorbornene (in agreement with a previous suggestion by Rebek et al.)<sup>9b</sup> to explain its lower reaction rate with respect to tetramethylethene.

We report here the results of a careful DFT study of the PFA epoxidation of these substrates. To have reference points that allow one to properly evaluate the results obtained with *anti*- and *syn*-sesquinorbornene, we also studied the PFA epoxidation of tetramethylethene as well as that of norbornene and norbornadiene (Scheme 2). The investigation of the latter derivatives was also warranted by the important role played by them in the study of the facial selectivity of organic reactions.<sup>10–12</sup>

## Computational Methods

Reactant (Figure 1) as well as transition structure (TS) geometries (Figures 2–5) for the reaction of PFA with norbornene, norbornadiene, tetramethylethene, and *anti*- and *syn*-

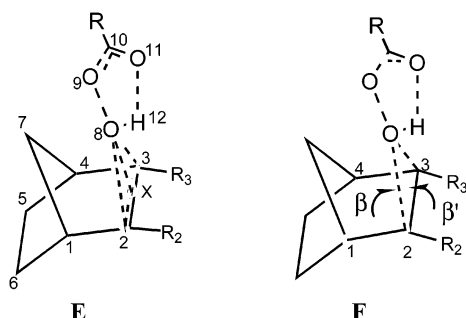
(8) Roof, A. A. M.; Winter, W. J.; Bartlett, P. D. *J. Org. Chem.* **1985**, *50*, 4093.

(9) (a) Koerner, T.; Slebocka-Tilk, H.; Brown, R. S. *J. Org. Chem.* **1999**, *64*, 196. (b) A “parallel” TS (corresponding to a planar TS) was previously suggested as favored for these systems by Rebek, J.; Marshall, L.; Wolak, R. *J. Org. Chem.* **1986**, *51*, 1649.

(10) (a) Brown, H. C.; Kawakami, J. H.; Ikegami, S. *J. Am. Chem. Soc.* **1970**, *92*, 6914. (b) Meinwald, J.; Labana, S. S.; Labana, L. L.; Wahl, Jr.; G. H. *Tetrahedron Lett.* **1965**, 1789.

(11) (a) Houk, K. N.; Rondan, N. G.; Brown, F. K. *Isr. J. Chem.* **1983**, *23*, 3. (b) Rastelli, A.; Bagatti, M.; Ori, A.; Gandolfi, R.; Burdisso, M. *J. Chem. Soc., Faraday Trans.* **1993**, *89*, 29 and references therein.

## SCHEME 3



sesquinorbornenes were fully optimized at the B3LYP/6-31G(d) and B3LYP/6-311+G(d,p) theory levels.<sup>13</sup> As for the basis set effect our results demonstrate that TS geometries do not, as a rule, heavily depend on the basis set used and only a slight increase of the forming bond lengths and of the intramolecular O<sub>11</sub>...H<sub>12</sub> distance is observed on passing from the 6-31G(d) to the larger 6-311+G(d,p) basis set. However, in two cases significant differences have been observed. Thus, the *syn,endo*-TS for norbornene epoxidation (*syn,endo*-1) is exactly spiro at the B3LYP/6-311+G(d,p) level, while a rotation of 20° away from the perpendicular orientation is present in the B3LYP/6-31G(d) transition structure.<sup>14</sup> In the *anti*-sesquinorbornene epoxidation, we found, at the B3LYP/6-31G(d) level, a highly distorted spiro-like TS that was not confirmed as a stationary point by B3LYP/6-311+G(d,p) calculations.<sup>14</sup> Notwithstanding these discrepancies the trends in geometries (and in electronic energies) obtained with the two basis sets are similar to each other and lead to the same conclusions. Therefore, only the B3LYP/6-311+G(d,p) data are reported and discussed here.

All calculations were performed with the Gaussian 98 suite of programs.<sup>15</sup> Critical points have been fully characterized by diagonalizing the Hessian matrixes of the optimized structures only at the B3LYP/6-31G(d) level; transition structures have RHF-UHF stable wave functions and only one negative eigenvalue (first-order saddle points). The corresponding eigenvector involves the expected O<sub>8</sub> oxygen approach to the double bond and the cleavage of the O<sub>8</sub>-O<sub>9</sub>, the lengthening of the C<sub>10</sub>=O<sub>11</sub>, and the shortening of the O<sub>9</sub>-C<sub>10</sub> peroxy acid bonds (see E in Scheme 3 for TS numbering).<sup>16</sup>

The B3LYP/6-311+G(d,p) TS geometries, with some relevant bond lengths, for PFA epoxidation of norbornene, norbornadiene, tetramethylethene, and *anti*-sesquinorbornene and *syn*-sesquinorbornenes are reported in Figures 2–5. Moreover, in addition to imaginary frequencies ( $\nu_i$ , cm<sup>-1</sup>) and dipole moments ( $\mu$ , D), the following angles (illustrated in F, Scheme 3) are reported for TSs of norbornene and norborna-

diene (Tables 1 and 2) and for tetramethylethene and *anti*- and *syn*-sesquinorbornene (Table 3) reactions.

(i)  $\alpha_2$  and  $\alpha_3$  that reflect pyramidalization of the C<sub>2</sub> and C<sub>3</sub> centers as a result of out-of-plane distortion of the R<sub>2</sub> and R<sub>3</sub> substituents. The absolute values are obtained from the corresponding improper torsion angles ( $|\alpha_2| = 180^\circ - |C_1-C_2-C_3-R_2|$  and  $|\alpha_3| = 180^\circ - |C_4-C_3-C_2-R_3|$ ) and are given positive (negative) sign when R<sub>2</sub> and R<sub>3</sub> substituent distortion takes place in the *anti* (*syn*) direction with respect to the methano bridge.

(ii)  $\beta$  and  $\beta'$ , namely, the dihedral angles between the forming oxirane plane and the mean C<sub>1</sub>-C<sub>2</sub>-C<sub>3</sub>-C<sub>4</sub> and R<sub>2</sub>-C<sub>2</sub>-C<sub>3</sub>-R<sub>3</sub> planes, respectively. A  $\beta$  value larger than  $\beta'$  means that the attacking oxygen is tilted away from the methano bridge.

(iii) The O<sub>8</sub>-X-C<sub>2</sub> angle that describes the oxygen approach geometry with respect to the center of the C=C bond (X is a dummy atom placed at the center of the C<sub>2</sub>-C<sub>3</sub> bond). A value smaller (larger) than 90° means that the O<sub>8</sub> is shifted toward (away from) the C<sub>2</sub> carbon atom.

(iv) The O<sub>9</sub>-O<sub>8</sub>-X angle that allows one to evaluate the alignment of the axis of the  $\pi$  cloud with the breaking O<sub>8</sub>...O<sub>9</sub> bond.

(v) The H<sub>12</sub>-O<sub>8</sub>-X-C<sub>2</sub> dihedral angle that defines the orientation of the O-H moiety with respect the C=C bond axis. The perfect spiro conformation corresponds to  $\pm 90^\circ$ , while a value of 0° corresponds to a planar array. Owing to the planarity of the peroxy acid moiety in all the reported TSs (out-of-plane distortion is always less than 3°), this angle practically corresponds to that between the peroxy acid plane and the C=C bond.

To produce theoretical activation parameters, vibrational frequencies in the harmonic approximation were calculated for all the optimized B3LYP/6-31G(d) structures and used, unscaled,<sup>17</sup> with the B3LYP/6-311+G(d,p) electronic energies to compute activation parameters (Tables 4 and 5).

The computed enthalpy, entropy, and free enthalpy were converted from the 1 atm standard state to the standard state of molar concentration (ideal mixture at 1 mol/L and 1 atm) to use them for a direct comparison with the experimental results in solution, where the latter activity scale is generally used.<sup>18,19</sup>

The contribution of solvent effects to the activation Gibbs free energies of the reactions under study were calculated via the self-consistent reaction field (SCRF) method using the CPCM model.<sup>20</sup> The solvation effect has been evaluated for dichloromethane (Tables 4 and 5), chloroform, and 1,2-dichloroethane (Table 6) solution by single-point calculation (i.e., with unrelaxed gas-phase reactant and TS geometries) at the B3LYP/6-31G(d) level and used to evaluate the B3LYP/6-311+G(d,p) Gibbs free energies in solution.

Reaction paths were analyzed by IRC calculations at the B3LYP/6-31G(d) level.<sup>21</sup>

(12) A computational study on the face selectivity of the epoxidation of norbornene and norbornadiene has been recently reported, but the authors limited their investigation to a pair of TSs for each substrate and used only the semiempirical AM1 method. Marchand, A. P.; Ganguly, B.; Shukla, R.; Krishnudu, Kumar, S.; Watson, W. H.; Bodige, S. G. *Tetrahedron* **1999**, *55*, 8313.

(13) (a) Becke, A. D. *J. Chem. Phys.* **1993**, *98*, 1372. (b) Lee, C.; Yang, W.; Parr, R. G. *Phys. Rev. B* **1988**, *37*, 785.

(14) Figures are reported in the Supporting Information.

(15) Gaussian 98, Revision A.6: M. J. Frisch, G. W. Trucks, H. B. Schlegel, G. E. Scuseria, M. A. Robb, J. R. Cheeseman, V. G. Zakrzewski, J. A. Montgomery, Jr., R. E. Stratmann, J. C. Burant, S. Dapprich, J. M. Millam, A. D. Daniels, K. N. Kudin, M. C. Strain, O. Farkas, J. Tomasi, V. Barone, M. Cossi, R. Cammi, B. Mennucci, C. Pomelli, C. Adamo, S. Clifford, J. Ochterski, G. A. Petersson, P. Y. Ayala, Q. Cui, K. Morokuma, D. K. Malick, A. D. Rabuck, K. Raghavachari, J. B. Foresman, J. Cioslowski, J. V. Ortiz, B. B. Stefanov, G. Liu, A. Liashenko, P. Piskorz, I. Komaromi, R. Gomperts, R. L. Martin, D. J. Fox, T. Keith, M. A. Al-Laham, C. Y. Peng, A. Nanayakkara, C. Gonzalez, M. Challacombe, P. M. W. Gill, B. Johnson, W. Chen, M. W. Wong, J. L. Andres, C. Gonzalez, M. Head-Gordon, E. S. Replogle, and J. A. Pople, Gaussian, Inc., Pittsburgh, PA, 1998.

(16) For the sake of simplicity the same numbering was used for norbornene, norbornadiene, and *anti*- and *syn*-sesquinorbornenes.

(17) Rastelli, A.; Bagatti, M.; Gandolfi, R. *J. Am. Chem. Soc.* **1995**, *117*, 4965.

(18) For conversion from the 1 atm standard state to the 1 mol/L standard state the following contributions need to be added to standard enthalpy, entropy, and free enthalpy:  $-RT$ ,  $-R - R \ln R/T$ , and  $RT \ln R/T$ , where  $R$  is the value of  $R$  in (L·atm)/(mol·K).<sup>19a</sup> For a reaction with  $A + B = C$  stoichiometry, the corrections for  $\Delta H^\ddagger$ ,  $\Delta S^\ddagger$ , and  $\Delta G^\ddagger$  are  $RT$ ,  $RT + RT \ln R/T$ , and  $-RT \ln R/T$ , respectively. Finally, at 278 K the corrections amount to 0.55 and  $-1.72$  kcal/mol for  $\Delta H^\ddagger$  and  $\Delta G^\ddagger$ , respectively, and 8.20 eu for  $\Delta S^\ddagger$ .<sup>17,19b</sup> To avoid misunderstanding, let us emphasize that the corrected theoretical data are still intended for gas-phase reactions.

(19) (a) Benson, S. *Thermochemical Kinetics*; Wiley: New York, 1968; p 8. (b) Jorgensen, W. L.; Lim, D.; Blake, J. F. *J. Am. Chem. Soc.* **1993**, *115*, 2936.

(20) (a) Cramer, C. J.; Truhlar, D. G. *Chem. Rev.* **1999**, *99*, 2161. (b) Barone, V.; Cossi, M. *J. Phys. Chem.* **1998**, *102*, 1995. (c) Tomasi, J.; Persico, M. *Chem. Rev.* **1994**, *94*, 2027. (d) Arnaud, R.; Adamo, C.; Cossi, M.; Milet, A.; Vallée, Y.; Barone, V. *J. Am. Chem. Soc.* **2000**, *122*, 324.

(21) Gonzales, C.; Schlegel, H. B. *J. Phys. Chem.* **1991**, *95*, 5853.



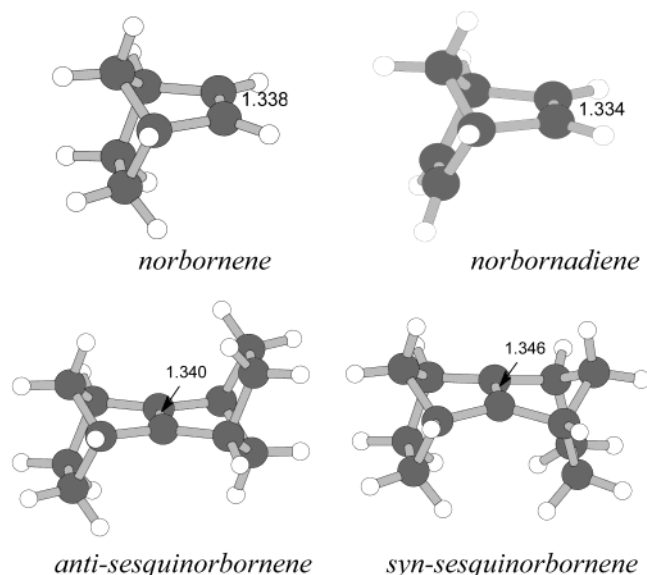


**FIGURE 1.** B3LYP/6-311+G(d,p) structure of norbornene, norbornadiene, and *anti*- and *syn*-sesquinorbornenes (bond lengths in angstroms).

## Results and Discussion

**Epoxidation of Norbornene and Norbornadiene with PFA.** The structure of norbornene and norbornadiene has computationally been investigated very thoroughly, in particular with HF and post-HF methods.<sup>22,23</sup> Our B3LYP/6-31G(d) data (Figure 1) confirm the previous results, in particular, of the out-of-plane distortion, *anti* with respect to the methano bridge, of the olefinic hydrogens. This deformation is twice as high in norbornene ( $\alpha = 7.1^\circ$ ) as in norbornadiene ( $\alpha = 3.3^\circ$ ) and does not change when the basis set is significantly improved [e.g., with the B3LYP/6-311+G(d,p) method the values are  $6.9^\circ$  and  $3.3^\circ$ , respectively]. The DFT geometries nicely reproduce the experimental values ( $7.3^\circ$  and  $3.7^\circ$ , for norbornene and norbornadiene, respectively),<sup>24,25</sup> which are similar to reported MP2/6-31G(d) data.<sup>22</sup>

For norbornene epoxidation we located the four possible transition structures arising from the *syn* and *anti* (relative to the methano bridge) attack by PFA, with *endo* (the peroxy acid hydrogen points inside) and *exo* orientation (*syn,exo-1*, *syn,endo-1*, *anti,exo-1*, and *anti,endo-1*, Figure 2 and Table 1). All of them feature a spiro approach with synchronous C---O bond formation. The planar peroxy acid moiety is perpendicular to the oxirane plane, while the O<sub>8</sub>---O<sub>9</sub> breaking bond is very well aligned with the  $\pi$  bond axis (O<sub>9</sub>---O<sub>8</sub>---X angle  $\approx 178^\circ$ ) at the center of the  $\pi$  system (O<sub>8</sub>---X---C<sub>2</sub>  $\approx 90^\circ$ ). Quite unexpectedly also *syn,endo-1* shows a symmetric spiro structure<sup>26</sup> in which the steric interactions between the peroxy acid and the methano bridge are lessened by an outside inclination of the forming oxirane ring. In fact, the  $\beta$  angle in *syn,endo-1* ( $115^\circ$ ) is higher than that ( $104^\circ$ ) in *syn,exo-1*. Also in the case of *anti,endo* attack steric

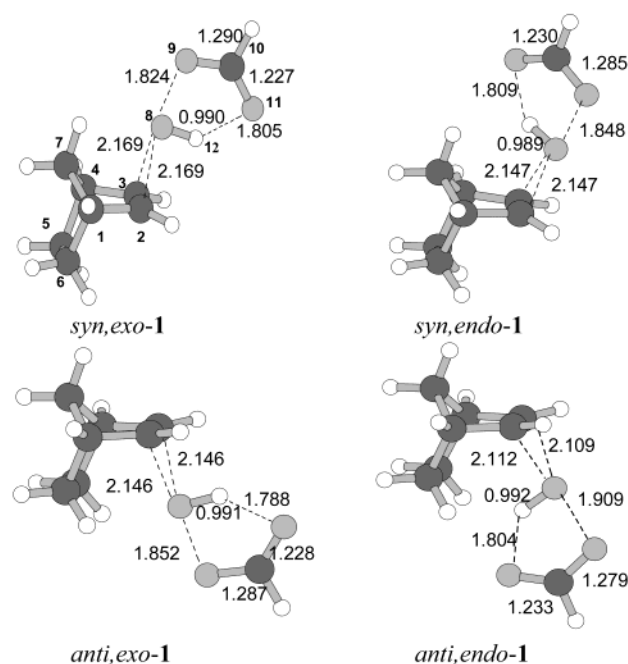


**FIGURE 2.** B3LYP/6-311+G(d,p) TSs for PFA epoxidation of norbornene (bond lengths in angstroms).

**TABLE 1.** Imaginary Frequencies ( $\nu_i$ ), Dipole Moments ( $\mu$ ), and Representative Angles (deg) for TSs 1 of the PFA Epoxidation of Norbornene at the B3LYP/6-311+G(d,p) Level<sup>a</sup>

param	<i>syn,exo-1</i>	<i>syn,endo-1</i>	<i>anti,exo-1</i>	<i>anti,endo-1</i>
$\nu_i$ (cm <sup>-1</sup> )	379	395	392	398
$\mu$ (D)	4.50	4.88	4.26	5.03
$\alpha$ (C <sub>2</sub> )	13.0	14.2	-7.7	-10.3
$\alpha$ (C <sub>3</sub> )	13.0	14.2	-7.7	-10.4
$\beta$	104.1	114.6	107.2	117.6
$\beta'$	88.8	79.6	80.5	72.6
O <sub>8</sub> ---X---C <sub>2</sub>	90.0	90.0	90.0	90.1
O <sub>9</sub> ---O <sub>8</sub> ---X	178.0	178.1	178.8	175.8
H <sub>12</sub> ---O---X---C <sub>2</sub>	90.0	-89.9	-90.0	89.7

<sup>a</sup> See the Computational Methods and Scheme 3 for numbering and angle definitions.

interactions are accommodated by an outside inclination of the oxirane ring, as supported by  $\beta = 118^\circ$  in *anti,endo-1* vs  $\beta = 107^\circ$  in *anti,exo-1*.

As for the olefinic hydrogens, *syn* attack promotes an increase in *anti* out-of-plane bending by  $6$ – $7^\circ$  ( $\alpha_2 = \alpha_3 \approx 13$ – $14^\circ$ ) relative to that of the former norbornene, while *anti* attack reverses the initial *anti* distortion of these hydrogens, giving rise to noticeable *syn* deformation ( $\alpha_2 = \alpha_3 = -8^\circ$  and  $-10^\circ$  in *anti,exo-1* and in *anti,endo-1*, respectively).

(26) In contrast with the symmetric spiro geometry of *syn,endo-1* located at the B3LYP/6-311+G(d,p) level, lower level B3LYP/6-31G(d) optimization leads to a TS with noticeable incipient C---O bond asynchrony ( $\Delta = 0.32$  Å) and a pronounced (by  $33^\circ$ ; H<sub>12</sub>---O<sub>8</sub>---X---C<sub>2</sub> =  $-123^\circ$ ) deviation from spiro orientation.<sup>14</sup> This observation suggests that steric interactions between the *endo*-oriented peroxy acid and the proximal hydrogen (at the norbornene methano bridge) are more influential with the smaller basis set. However, notwithstanding the H<sub>12</sub>---O<sub>8</sub>---X---C<sub>2</sub> angle changes by  $30^\circ$  on passing from the B3LYP/6-31G(d) to the B3LYP/6-311+G(d,p) structure, the energy obtained by single-point B3LYP/6-311+G(d,p) calculation on the lower level structure is very similar (only 0.3 kcal/mol higher) to that of the fully optimized B3LYP/6-311+G(d,p) structure. That is, distortion away from an ideal spiro orientation is quite easy.

(22) Koch, W.; Holthausen, M. C. *J. Phys. Chem.* **1993**, *97*, 10021 and references therein.

(23) Williams, R. V.; Colvin, M. E.; Tran, N.; Warrenner, R. N.; Margetic, D. *J. Org. Chem.* **2000**, *65*, 562.

(24) Ermer, O.; Bell, P.; Mason, S. A. *Angew. Chem.* **1989**, *101*, 1298.

(25) Knuchel, G.; Grassi, G.; Vogelsanger, B.; Bauder, A. *J. Am. Chem. Soc.* **1993**, *115*, 10845.

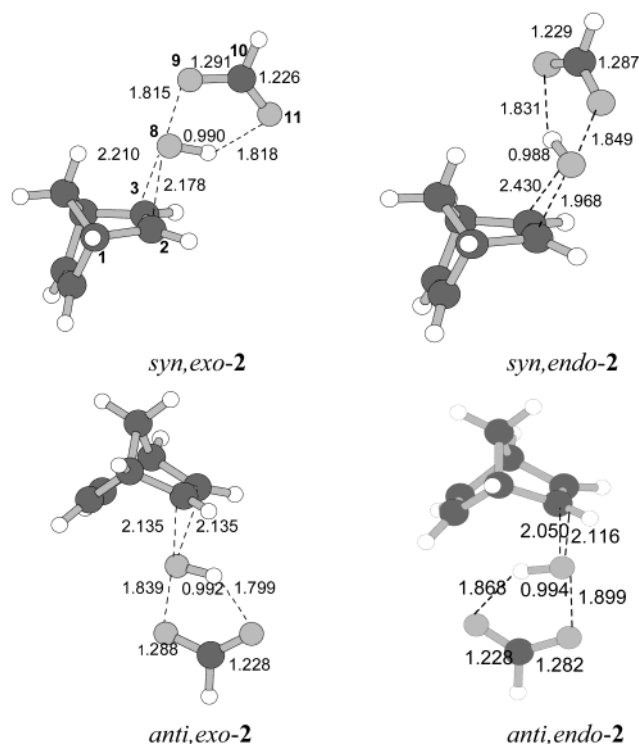


**FIGURE 3.** B3LYP/6-311+G(d,p) TSs for PFA epoxidation of norbornadiene (bond lengths in angstroms).

Houk has stressed that torsional strain involving the incipient bonds and the allylic bonds can play a dominant role in driving face selectivity in these systems.<sup>11a</sup> This effect has been suggested to favor *syn* attack, for example, in 1,3-dipolar cycloadditions to norbornene, since staggering is much better (and torsional strain much lower) for *syn* than for *anti* attack.<sup>11a</sup> The latter observation holds also for peroxy acid epoxidation of norbornene notwithstanding the different geometry of the forming bonds in the two kinds of reactions. In fact, the absolute value of the torsional angle between the incipient bonds and the methano bridge C–C bonds in TSs *syn-1* is larger ( $|C_7-C_1-C_2-O_8| \approx |C_7-C_4-C_3-O_8| \approx 43-45^\circ$ ) than the corresponding angle involving the forming bonds and the allylic bonds of the ethano bridge in TSs *anti-1* ( $|C_6-C_1-C_2-O_8| \approx |C_5-C_4-C_3-O_8| \approx 7-9^\circ$ ). Furthermore, also the staggering between the bridgehead and the vinyl hydrogens is higher in TSs *syn-1* ( $|H_1-C_1-C_2-H_2| \approx 32^\circ$ ) than that in their *anti-1* ( $\sim 9-12^\circ$ ) counterparts. These data suggest that torsional strain can be operative as one of the controlling factors of face selectivity of norbornene epoxidation reactions. This factor has already been suggested to be at work in the epoxidation of cyclohexene derivatives<sup>4b</sup> and 1,2-dihydronaphthalenes.<sup>27</sup>

Also for norbornadiene epoxidation we located four TSs, namely, *syn,exo-2*, *syn,endo-2*, *anti,exo-2*, and *anti,endo-2* (Figure 3 and Table 2). Three of them, *syn,exo-2*, *anti,exo-2*, and *anti,endo-2*, are similar to the corresponding norbornene TSs, even if they are slightly asynchronous ( $\Delta = 0.03-0.07$  Å), but *syn,endo-2* appears quite different from its norbornene counterpart. Interestingly,

**TABLE 2.** Imaginary Frequencies ( $\nu_i$ ), Dipole Moments ( $\mu$ ), and Representative Angles (deg) for TSs **2** of the PFA Epoxidation of Norbornadiene at the B3LYP/6-311+G(d,p) Level<sup>a</sup>

param	<i>syn,exo-2</i>	<i>syn,endo-2</i>	<i>anti,exo-2</i>	<i>anti,endo-2</i>
$\nu_i$ (cm <sup>-1</sup> )	371	400	400	414
$\mu$ (D)	4.18	4.68	4.11	5.15
$\alpha(C_2)$	11.9	22.7	-9.5	-9.7
$\alpha(C_3)$	11.8	6.1	-9.5	-13.3
$\beta$	105.7	111.9	107.1	115.1
$\beta'$	85.7	82.6	82.5	76.4
O <sub>8</sub> -X-C <sub>2</sub>	88.7	71.5	90.0	87.4
O <sub>9</sub> -O <sub>8</sub> -X	179.5	176.5	179.5	175.7
H <sub>12</sub> -O-X-C <sub>2</sub>	91.5	-151.0	90.0	94.0

<sup>a</sup> See footnote *a* in Table 1.

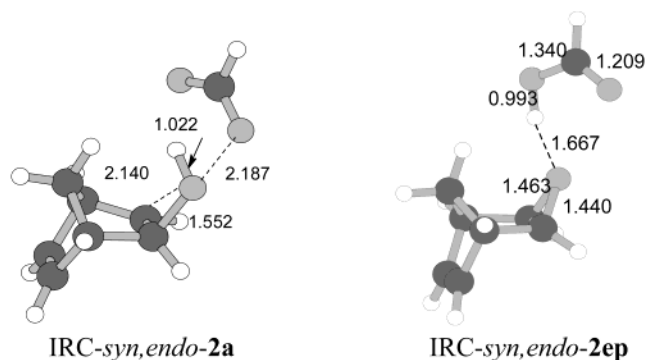


**FIGURE 4.** Representative B3LYP/6-31G(d) IRC points from TS *syn,endo-2* for the PFA epoxidation of norbornadiene (bond lengths in angstroms).

the latter TS shows so large a deviation from spiro geometry (by  $61^\circ$ ;  $H_{12}-O_8-X-C_2 = -151^\circ$ ) that it can be classified as planar-like. Incipient bond length asynchrony is quite strong ( $\Delta = 0.46$  Å) and gives rise to a sizable difference in the pyramidalization of the reacting olefinic carbons ( $\alpha_2 = 23^\circ$  and  $\alpha_3 = 6^\circ$ ), while the approach trajectory is shifted toward the C<sub>2</sub> center ( $O_8-C_2-C_3 = 91^\circ$ ). It is quite evident that in this TS the bonding interaction with one (C<sub>2</sub>) of the two reacting olefinic carbons is considerably privileged over that with the other one (C<sub>3</sub>). Formation of the partial positive charge at C<sub>3</sub> (involved in the longer incipient bond), as a result of asynchrony in oxirane bond formation, can be assisted by through-space electron donation by the non-reacting double bond.<sup>28</sup>

IRC going downhill from TS *syn,endo-2* to the final *syn*-epoxide reveals an interesting behavior. The considerable asynchrony present at TS *syn,endo-2* increases further for a while along the descent to epoxide. That is, formation of one of the two C–O bonds almost goes to completion before that of the other has hardly started, as clearly illustrated by IRC-*syn,endo-2a* (Figure 4). This IRC point, with its strong incipient bond length asynchrony ( $\Delta = 0.6$  Å) and the value of the O<sub>8</sub>-C<sub>2</sub>-C<sub>3</sub> angle of  $92^\circ$ , looks like the result of attack by an OH<sup>+</sup> particle, assisted by the formate counterion, at the norbornadiene C<sub>2</sub> center with formation of a positive charge at C<sub>3</sub>. IRC correctly terminates with a hydrogen-bonded complex between the *syn*-epoxide and formic acid (namely, IRC-

(27) Lucero, M. J.; Houk, K. N. *J. Org. Chem.* **1998**, *63*, 6973.

(28) March, J. *Advanced Organic Chemistry: Reactions, Mechanisms, and Structure*; Wiley-Interscience: New York, 1985; p 312.

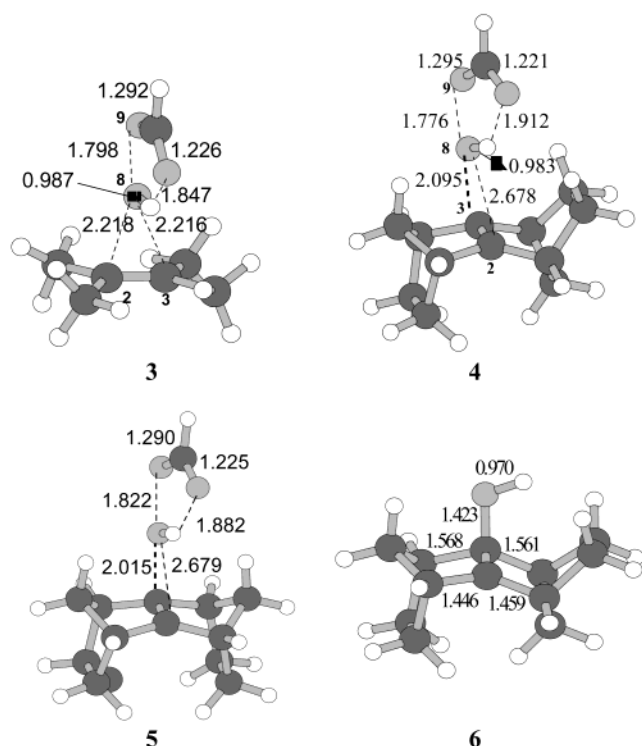


**FIGURE 5.** B3LYP/6-311+G(d,p) TSs for PFA epoxidation of tetramethylethene (**3**), *anti*-sesquinorbornene (**4**), and *syn*-sesquinorbornene (**5**) and B3LYP/6-31G(d) geometry of  $\alpha$  hydroxy carbocation **6** (bond lengths in angstroms).

**TABLE 3.** Imaginary Frequencies ( $\nu_i$ ), Dipole Moments ( $\mu$ ), and Representative Angles (deg) for TSs **3–5** of the PFA Epoxidation of Tetramethylethene, and *anti*- and *syn*-sesquinorbornenes, Respectively, at the B3LYP/6-311+G(d,p) Level<sup>a</sup>

param	<b>3</b>	<b>4</b>	<b>5</b>
$\nu_i$ (cm <sup>-1</sup> )	377	375	372
$\mu$ (D)	3.97	4.30	5.01
$\alpha(C_2)$	7.9	23.6	18.2
$\alpha(C_3)$	7.9	30.9	25.9
$\beta$	97.6	98.6	101.0
$\beta'$	90.3	108.5	101.0
O <sub>8</sub> –X–C <sub>2</sub>	89.9	116.0	119.7
O <sub>9</sub> –O <sub>8</sub> –X	179.5	173.8	173.9
H <sub>12</sub> –O–X–C <sub>2</sub>	90.0	10.1	0.0

<sup>a</sup> See footnote *a* in Table 1.

*syn,endo-2ep*, Figure 4). Therefore, calculations suggest that a “one-step nonconcerted” mechanism via a planar-like TS can be at work for the *syn,endo* PFA attack on norbornadiene.<sup>29</sup>

Since a very similar behavior is suggested by calculations for the PFA epoxidation of sesquinorbornene derivatives, more detailed comments are deferred until later.

**Epoxidation of Tetramethylethene with PFA.** The TS located by us for the reaction of PFA with tetramethylethene (TS **3**, Figure 5 and Table 3) is similar in every respect to that reported previously for the reaction

of PFA with ethene,<sup>2a,3a</sup> the only significant difference being slightly higher forming bond lengths. In particular, the synchrony and spiro geometry of **3** testify to the fact that the presence of carbon centers that can easily bear a positive charge is not enough to trigger asynchrony in incipient bond lengths. Having thus established that a “normal” symmetrically tetrasubstituted double bond is intrinsically a well-behaved system, i.e., a system that prefers a spiro synchronous geometry, we can address the reaction of PFA with “particular” alkenes such as *anti*- and *syn*-sesquinorbornenes.

**Epoxidation of *anti*- and *syn*-Sesquinorbornene with PFA.** Theoretical calculations [HF/6-31G(d) and MP2/6-31G(d)]<sup>22</sup> strongly support a planar array ( $\alpha = 0^\circ$ ) of atoms for the double bond of *anti*-sesquinorbornene<sup>30,31</sup> but also suggest [HF/6-31G(d) calculations] that the out-of-plane bending in this system is very easy. Experimental structural data (for derivatives of *syn*-sesquinorbornene)<sup>30,31</sup> and computational data<sup>22</sup> have unambiguously demonstrated that the double bond of *syn*-sesquinorbornene is strongly pyramidalized [ $\alpha = 16^\circ$  at the MP2/6-31G(d) level].<sup>22</sup> The energy necessary to change the  $\alpha$  angle, with respect to the equilibrium value, however, is somewhat larger in *syn*-sesquinorbornene than in *anti*-sesquinorbornene [HF/6-31G(d)].<sup>22</sup> In *syn*-sesquinorbornene steric repulsion between the two ethano bridges counteracts the intrinsic tendency of *anti* (with respect to the methano bridges) out-of-plane deformation of the double bond. The increase in energy due to steric crowding increases rapidly from the equilibrium geometry onward.

Our B3LYP/6-311+G(d,p) calculations fully confirm these data, indicating a planar structure for *anti*-sesquinorbornene and a pyramidalized one for the *syn*-isomer ( $\alpha = 15^\circ$ ). The latter is predicted to be more stable than the former by 2.7 kcal/mol.

As recently suggested by Brown et al.,<sup>9a</sup> it is quite evident that for steric reasons these two alkenes can accommodate a planar transition structure, for the epoxidation with peroxy acids, much more easily than a spiro TS.

A careful B3LYP/6-311+G(d,p) search led us to locate only one transition structure for the PFA epoxidation of *anti*-sesquinorbornene, namely, TS **4**, which provides an example of a “planar-like” TS since it differs from an ideal planar orientation by only  $\sim 10^\circ$  (H<sub>12</sub>–O<sub>8</sub>–X–C<sub>2</sub> =  $10.1^\circ$ , with the peroxy acid plane rotated toward the *syn* ethane bridge).<sup>32</sup> This planar-like arrangement is accompanied by a very high asynchrony in bond formation ( $\Delta = 0.58$  Å) which is significantly larger than that in *syn,endo-2* ( $\Delta = 0.46$  Å), and the average incipient bond length of **4** (2.39 Å) is higher compared to those of both *syn,endo-2* (2.20 Å) and **3** (2.22 Å). Pyramidalization of both the olefinic carbon centers of TS **4** is quite pronounced ( $\alpha_2 = 24^\circ$  and  $\alpha_3 = 31^\circ$ ), and consistently, the larger one corresponds to the center involved in the shorter incipient bond.

Moreover, the O<sub>8</sub>–X–C<sub>2</sub> angle is much higher than  $90^\circ$  (i.e.,  $116^\circ$ ) and the O<sub>8</sub>–C<sub>3</sub>–C<sub>2</sub> angle significantly larger

(29) IRC analysis shows that in the case of the *syn,exo* attack synchronous C–O bond formation uniformly proceeds along all the reaction coordinates, from reactants via TS *syn,exo-2* to the final epoxide.

(30) Gajhede, M.; Jorgensen, F. M.; Kopecky, K. R.; Watson, W.; Kashyap, R. P. *J. Org. Chem.* **1985**, *50*, 4395.

(31) Paquette, L. A.; Kunzer, H.; Green, K. E.; De Lucchi, O.; Licini, G.; Pasquato, L.; Valle, G. *J. Am. Chem. Soc.* **1986**, *108*, 3453 and references therein.



than 90° (i.e., 99°), thus indicating that the approach of the electrophilic peroxy system follows a trajectory tilted outside with respect to the *anti*-sesquinorbornene double bond. The attacking oxygen atom (O<sub>8</sub>) lies slightly outside with respect to the C<sub>3</sub> carbon atom, with which it interacts more strongly, and, consequently, far away from the other olefinic carbon (C<sub>2</sub>). Different bonding interactions are also reflected in the Wiberg bond index<sup>33</sup> that is much higher for the shorter forming bond (0.32 for O<sub>8</sub>---C<sub>3</sub>) than for the longer one (0.13 for O<sub>8</sub>---C<sub>2</sub>).

Thus, one may confidently argue that TS **4** is an example of a nonconcerted TS with significant bond formation at only one of the olefinic centers, while bonding interaction with the other unsaturated carbon center is negligible.<sup>34,35</sup>

To corroborate this statement and clarify the concertedness problem, we followed, by IRC-B3LYP/6-31G(d) calculations, the geometry changes that progressively take place in **4** on its way downhill to the final epoxide. Some significant points of this pathway are illustrated in Figure 6. The first point reported, IRC-**4a** not far from the TS, has the following noteworthy features: (i) a short C<sub>3</sub>---O<sub>8</sub> bond that stands in striking contrast with a long C<sub>2</sub>---O<sub>8</sub> distance (the incipient bond asynchrony in IRC-**4a** increases to  $\Delta = 0.90$  Å from  $\Delta = 0.59$  Å in B3LYP/6-31G(d) TS **4**), (ii) the Wiberg index of the C<sub>3</sub>---O<sub>8</sub> bond (0.89) suggests an almost completely formed bond, while the C<sub>2</sub>---O<sub>8</sub> index (0.17) is only imperceptibly higher than that in the TS, (iii) the O<sub>8</sub>---C<sub>3</sub>---C<sub>2</sub> and O<sub>8</sub>---C<sub>2</sub>---C<sub>3</sub> angles (107° and 120°, respectively) not only are significantly larger than 90° but are higher than the corresponding ones in the TS (98° and 116°, respectively), (iv) the O—H bond points toward C<sub>2</sub>. All these data strongly suggest

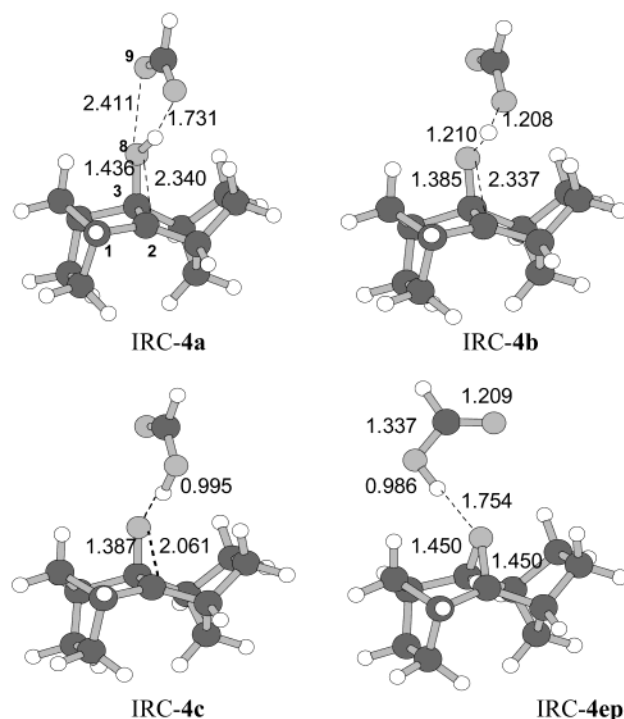


**FIGURE 6.** Representative B3LYP/6-31G(d) IRC points from TS **4** for the PFA epoxidation of *anti*-sesquinorbornene (bond lengths in angstroms).

that, at this IRC point, there is hardly any bonding interaction between O<sub>8</sub> and C<sub>2</sub> while the C<sub>3</sub>---O<sub>8</sub> bond is almost completely formed. Moreover, two successive points, IRC-**4b** and IRC-**4c**, nicely demonstrate that the C<sub>2</sub>---O<sub>8</sub> bond formation takes place only after the proton has been completely transferred to the formate anion to eventually produce hydrogen-bonded epoxide (IRC-**4ep**). We can conclude that, in the PFA epoxidation of *anti*-sesquinorbornene, formation of one of the oxirane C—O bonds takes place first while that of the second one commences afterward, in a nonconcerted process.<sup>36,37</sup>

The hydroxysesquinorbornene moiety of IRC-**4a** closely resembles that of the  $\alpha$ -hydroxy carbocation **6** (Figure 5; the Wiberg indices for C<sub>3</sub>—OH and C<sub>2</sub>---OH are 0.93 and 0.10, respectively). IRC-**4a** can properly be described as an  $\alpha$ -hydroxy carbocation with the OH group hydrogen-bonded to a formate anion. Stabilization of the positive charge in **6** and IRC-**4a** can be assisted by  $\sigma$  delocalization.<sup>28,38</sup> However, IRC-**4a**, in contrast with  $\alpha$ -hydroxy

(32) Optimization at the B3LYP/6-31G(d) level led to a further TS (a fully characterized first-order saddle point) that exhibits a spiro-like orientation, with the hydrogen peroxy acid directed toward the methano bridge (H<sub>12</sub>—O<sub>8</sub>—X—C<sub>2</sub> = -114°), accompanied by a considerable asynchrony ( $\Delta = 0.375$  Å) in C—O bond formation.<sup>14</sup> In this asynchronous TS the O—H bond is closer to the shorter forming bond in contrast with what is observed for asynchronous planar-like TSs *syn,endo*-**2**, -**4**, and -**5** but also with asynchronous spiro-like TSs such as **D'** (in all these TSs the O—H bond is closer to the longer forming bond). B3LYP/6-31G(d) IRC analysis, on the product side, indicates that the final epoxide (hydrogen-bonded to the formic acid) is formed in a nonconcerted one-step process. It resides higher in energy than TS **4**. However, we were not able to locate this TS with the higher basis set: 6-311+G(d,p) optimization starting from the 6-31G(d) geometry led to the planar TS **4**.

(33) Wiberg, K. B. *Tetrahedron* **1968**, *24*, 1083.

(34) (a) According to Lowe “the word concerted is meaningless unless we state what the two processes (the reference processes) are that occur simultaneously”, and when “one process takes place first and the second one commences afterwards”, the mechanism must be labeled “nonconcerted”.<sup>35</sup> Consequently, the process under study is nonconcerted as far as the timing of the two oxirane C—O bond formations is concerned. (b) Two reviewers emphasized that it might be better to keep the term “concerted” or “nonconcerted” for the absence or the presence, respectively, of an intermediate before the product formation. We feel that the terms “one-step” and “stepwise” are more adequate to describe these two possibilities while the terms “concerted” (that can be either “synchronous” or “asynchronous”) and “nonconcerted” properly describe the bond timing. A concerted process necessarily corresponds to a one-step stereospecific (configuration retention) mechanism that follows, in the case of pericyclic reactions, the Woodward–Hoffmann (W–H) rules. A nonconcerted pathway can be either a stepwise (with possible configuration loss) or a one step pathway. It is interesting to emphasize that the stereochemical outcome of one-step nonconcerted processes is not controlled by W–H rules as nicely exemplified by the preference for the orbital symmetry forbidden stereochemistry exhibited by the 1,5-sigmatropic shift of substituted norcardiene systems (Kless, A.; Nendel, M.; Wilsey, S. Houk, K. N. *J. Am. Chem. Soc.* **1999**, *121*, 4524).

(35) Lowe, J. P. *J. Chem. Educ.* **1974**, *51*, 785–786.

(36) Interestingly, the nonconcerted C—O bond formation in a one-step process via a planar TS, disclosed by IRC analysis, was anticipated by Rebek et al., on the basis of intuitive chemical reasoning.<sup>9b</sup> A mechanism that corresponds to a nonconcerted one-step process via a planar TS was also suggested by Hanzlik et al. for the peroxy acid epoxidation of styrene derivatives.<sup>6b</sup>

(37) A word of caution is in order as far as the chemical significance of IRC paths is concerned. One must always keep in mind that the meaning and theoretical status of IRC points is different from that of stationary points (minima and first-order saddle point) and avoid temptation to attribute excessive chemical significance to them. The IRC coordinate corresponds to the minimum energy path located in mass-weighted coordinates and is the path traced by a classical particle sliding from a saddle point down to a minimum with zero kinetic energy. It is a path on the potential energy surface, not a true trajectory: real molecules have kinetic energy and will not follow the intrinsic reaction path. Anyway, at present, IRC represents the more convenient description of the reaction mechanisms as they are qualitatively treated by organic chemists.

carbocation **6**, is not a minimum on the potential energy surface given that the proton transfer from the  $\alpha$ -hydroxy carbocation moiety to the formate anion can occur without any activation energy. That is, the epoxidation of *anti*-sesquinorbornene is a one-step process without formation of intermediates.

In conclusion, the *anti*-sesquinorbornene epoxidation via the planar-like TS **4** provides a computational example of a one-step nonconcerted reaction. We have recently demonstrated, with DFT calculations, that this kind of mechanism can be operative for the oxygen insertion in the alkane C–H bond by trifluoroperoxyacetic acid.<sup>39</sup>

It is well established that attacks (by peroxy acids, 1,3-dipoles, etc.) on *syn*-sesquinorbornene take place from the top side of the molecule, *syn* relative to the methano bridges.<sup>8</sup> For this kind of attack we managed to locate, with B3LYP/6-311+G(d,p) calculations, only one first-order saddle point, namely, TS **5** (Figure 5 and Table 3), that has an *exactly planar* ( $H_{12}-O_8-X-C_2=0^\circ$ ) geometry with the O–H bond pointing inside and eclipsing the C=C bond. Incipient bond asynchrony in **5** ( $\Delta = 0.66 \text{ \AA}$ ,  $O_8-X-C_2 = 120^\circ$ ,  $O_8-C_3-C_2 = 102^\circ$ ) is even more pronounced than in **4** ( $0.58 \text{ \AA}$ ,  $O_8-C_3-C_2 = 99^\circ$ ). The pyramidalization of the two olefinic centers in **5** ( $\alpha_2 = 18^\circ$  and  $\alpha_3 = 26^\circ$ ) is lower than that in **4** even if, in contrast to the planar double bond of *anti*-sesquinorbornene, that of *syn*-sesquinorbornene is strongly pyramidalized. The planar double bond of *anti*-sesquinorbornene can easily undergo a large out-of-plane deformation (as discussed at the beginning of this section), while the further out-of-plane *anti* bending of the pyramidalized *syn*-sesquinorbornene double bond, promoted by the peroxy acid attack, is evidently counteracted by a sizable increase in steric repulsion between the two ethano bridges, facing each other in the bottom half of the molecule.

IRC going from planar TS **5** toward the final epoxide fully parallels the corresponding one mentioned for planar-like TS **4**. Moreover, all the observations reported above for TS **4** also hold for TS **5**: *syn*-sesquinorbornene epoxidation provides a further convincing example of a nonconcerted one-step process via a planar TS, thus confirming the viability of this mechanism.

**Energetics of Norbornene Derivate Epoxidation. Computational Prediction vs Experimental Data.** The activation parameters for the PFA epoxidation of norbornene, norbornadiene, tetramethylethene, and *anti*- and *syn*-sesquinorbornenes, in the gas phase and dichloromethane solution at 298.15 K, are reported in Tables 4–6, while the computational activation free energies under the same conditions used in kinetic experiments are collected in Table 7.

Inspection of Table 4 shows that in the case of norbornene both the *syn*-TSs are predicted to be considerably more stable than their *anti* counterparts, and this difference in energy easily explains the complete *syn*

**TABLE 4. Electronic Activation Energies ( $\Delta E^\ddagger$ ), Enthalpies ( $\Delta H^\ddagger$ ), Entropies ( $\Delta S^\ddagger$ ), and Free Energies [ $\Delta G^\ddagger$  (Gas Phase) and  $\Delta G^\ddagger_{CH_2Cl_2}$  (Dichloromethane Solution)] for PFA Epoxidation of Norbornene**

TS	$\Delta E^\ddagger$ <sup>a</sup>	$\Delta H^\ddagger$ <sup>b</sup>	$\Delta S^\ddagger$ <sup>b</sup>	$\Delta G^\ddagger$ <sup>b</sup>	$\Delta G^\ddagger_{CH_2Cl_2}$ <sup>c</sup>
<i>syn,exo-1</i>	9.88	10.48	−25.93	18.22	17.95
<i>syn,endo-1</i>	11.00	11.62	−28.61	20.15	19.93
<i>anti,exo-1</i>	12.85	13.54	−30.02	22.50	22.66
<i>anti,endo-1</i>	15.34	15.95	−27.74	24.23	24.02

<sup>a</sup> Electronic energies from B3LYP/6-311+G(d,p) calculations. Energies (hartrees): norbornene, −272.799542; peroxyformic acid, −264.972914; *syn,exo-1*, −537.756706. <sup>b</sup> For evaluation of the thermodynamic properties the B3LYP/6-31G(d)-computed kinetic contributions are used. Energies in kcal/mol, entropy in cal/(mol K). Standard state (298.15 K) of the molar concentration scale (gas in an ideal mixture at 1 mol/L and  $P = 1 \text{ atm}$ ). <sup>c</sup> Solvent (dichloromethane) effect evaluated with the CPCM model at the B3LYP/6-31G(d) level.

**TABLE 5. Electronic Activation Energies ( $\Delta E^\ddagger$ ), Enthalpies ( $\Delta H^\ddagger$ ), Entropies ( $\Delta S^\ddagger$ ), and Free Energies [ $\Delta G^\ddagger$  (Gas Phase) and  $\Delta G^\ddagger_{CH_2Cl_2}$  (Dichloromethane Solution)] for PFA Epoxidation of Norbornadiene**

TS	$\Delta E^\ddagger$ <sup>a</sup>	$\Delta H^\ddagger$ <sup>b</sup>	$\Delta S^\ddagger$ <sup>b</sup>	$\Delta G^\ddagger$ <sup>b</sup>	$\Delta G^\ddagger_{CH_2Cl_2}$ <sup>c</sup>
<i>syn,exo-2</i>	9.54	10.22	−25.55	17.84	17.64
<i>syn,endo-2</i>	10.90	11.54	−26.84	19.56	19.36
<i>anti,exo-2</i>	12.67	13.23	−27.38	21.40	20.92
<i>anti,endo-2</i>	12.94	13.33	−25.58	20.96	19.93

<sup>a</sup> Electronic energies from B3LYP/6-311+G(d,p) calculations. Energies (hartrees): norbornadiene, −271.549963; *syn,exo-2*, −536.507671. <sup>b,c</sup> See footnotes *b* and *c* in Table 4. The symmetry number ( $\sigma$ ) used to calculate the norbornadiene entropy is 2.

**TABLE 6. Electronic Activation Energies ( $\Delta E^\ddagger$ ), Enthalpies ( $\Delta H^\ddagger$ ), Entropies ( $\Delta S^\ddagger$ ), and Free Energies [ $\Delta G^\ddagger$  (Gas Phase) and  $\Delta G^\ddagger_{CH_2Cl_2}$  (Dichloromethane Solution)] for PFA Epoxidation of Tetramethylethylene (**3**) and *anti*- (**4**) and *syn*-Sesquinorbornene (**5**)**

TS	$\Delta E^\ddagger$ <sup>a</sup>	$\Delta H^\ddagger$ <sup>b</sup>	$\Delta S^\ddagger$ <sup>b</sup>	$\Delta G^\ddagger$ <sup>b</sup>	$\Delta G^\ddagger_{CH_2Cl_2}$ <sup>c</sup>
<b>3</b>	7.33	7.75	25.67	15.41	16.46
<b>4</b>	10.49	11.04	−31.12	19.22	21.42
<b>5</b>	8.99	9.63	−29.64	18.48	18.86

<sup>a</sup> Electronic energies from B3LYP/6-311+G(d,p) calculations. Energies (hartrees): tetramethylethene, −235.923698; *anti*-sesquinorbornene, −466.969274; *syn*-sesquinorbornene, −466.973595; **3**, −500.884930; **4**, −731.925477; **5**, −731.932187. <sup>b,c</sup> See footnotes *b* and *c* in Table 4. The symmetry numbers ( $\sigma$ ) used to calculate the entropy are 4 for tetramethylethene, 2 for *anti*- and *syn*-sesquinorbornene, and 1 for all TSs. A further correction of  $R \ln 2$  to  $\Delta S^\ddagger$  is added for the reactions of *anti*-sesquinorbornene as enantioprotic attacks are not experimentally distinguishable.

selectivity observed experimentally.<sup>10a</sup> Several factors (steric, hyperconjugative, etc., in addition to torsional effects) inextricably concur in determining this result for the peroxy acid epoxidation in a way similar to that suggested for other norbornene reactions, such as 1,3-dipolar cycloadditions.<sup>11,22</sup> Notice how the favor in energy of *exo*-TSs over their *endo* counterparts is far from being dramatic.

Also in the case of norbornadiene epoxidation calculations predict a dominant *syn* selectivity, once again in accord with the experiment,<sup>10b</sup> even if the energy difference between *syn* and *anti* attack is, with respect to norbornene, attenuated. For this reaction calculations predict that the *exo* orientation should prevail over the *endo* one in the *syn* attack while *endo* and *exo* orientations should compete in a balanced way in the case of

(38) Stabilization of the positive charge in **6** by  $\sigma$  delocalization is supported by the observation that it is 6.0 kcal/mol more stable than the corresponding protonated epoxide, while the protonated epoxide deriving from tetramethylethene resides 1.3 kcal/mol lower in energy than the related open  $\alpha$ -hydroxy carbocation.

(39) Freccero, M.; Gandolfi, R.; Sarzi-Amade M.; Rastelli, A. *Tetrahedron* **2001**, 57, 9843.



**TABLE 7. Comparison between the Experimental ( $\Delta G_{\text{exptl}}$ ) and Theoretical ( $\Delta G_{\text{theor}}^\ddagger$ )<sup>a</sup> Data for Peroxy Acid Epoxidation of Norbornene,<sup>b</sup> Norbornadiene,<sup>b</sup> Tetramethylethene, and *anti*- and *syn*-Sesquinornbornene**

olefin	$\Delta G_{\text{theor}}^\ddagger$	$\Delta G_{\text{exptl}}$
norbornene (273.6 K in chloroform) <sup>10b</sup>	17.00	17.39
norbornadiene (273.6 K in chloroform) <sup>10b</sup>	16.69	17.36
tetramethylethylene (298.15 K in dichloroethane) <sup>9a</sup>	15.86	16.17
<i>syn</i> -sesquinornbornene (at 298.15 K in dichloroethane)	18.16	16.93 <sup>c</sup>
<i>anti</i> -sesquinornbornene (at 298.15 K in dichloroethane) <sup>9a</sup>	20.07	17.40

<sup>a</sup> Electronic energies from B3LYP/6-311+G(d,p) calculations. Contribution of molecular motions and solvent effect (CPCM model) from B3LYP/6-31G(d) calculations. <sup>b</sup> The reaction rate, and the corresponding free activation energy, of norbornene and norbornadiene reaction is determined almost exclusively by the reaction channel via TSs *syn,exo-1* and *syn,exo-2*, respectively. <sup>c</sup> This value has been evaluated on the basis of a reaction rate constant ratio ( $k_{\text{syn}}/k_{\text{anti}}$ ) of 2.2 reported by Bartlett et al.<sup>8</sup>

*anti* attack, with *anti,endo-2* slightly more stable (~1 kcal/mol) than *anti,exo-2*. The latter observation can be traced back to a destabilizing interaction between the lone pairs of the peroxy acid peroxy oxygens and the distal  $\pi$ -bond in *anti,exo-2* and to attraction between the hydrogen of the OH group and the same double bond in *anti,endo-2*.

The experimental kinetic studies<sup>10b</sup> on the MCPBA epoxidation of norbornene and norbornadiene in chloroform at 0.5° indicate that they are epoxidated at a comparable rate, and this finding is reasonably well reproduced by calculations. In fact the experimental activation free energies for both reactions compare well with the theoretical predictions (Table 7) that, however, seem to slightly overestimate the reactivity of norbornadiene.

The capability of DFT calculations in reproducing experimental results is confirmed by the observation that calculations manage not only to reproduce the experimental reactivity trend in the case of tetrasubstituted alkenes, with reactivity in the order tetramethylethylene > *syn*-sesquinornbornene > *anti*-sesquinornbornene (Table 6), but also to produce free activation energies that are similar to the experimental ones (with a slight reactivity underestimation, in particular in the case of *anti*-sesquinornbornene) (Table 7). The substantial accord between the computational and experimental data validate the DFT methods used in our study as adequate to deal with the reactivity of sesquinornbornene derivatives.

Thus, we can confidently hope that the planar transition structures disclosed by calculations are not an artifact of the method used but that they are “true” TS geometries for epoxidations of this kind of substrate.

## Conclusion

Our B3LYP/6-311+G(d,p) study on the peroxy acid epoxidation of norbornene derivatives demonstrates the viability of reaction pathways that go through planar (the peroxy acid and the reacting C=C bond lie in the same plane) or planar-like TSs at variance with what is the more common choice of spiro TSs (the peroxy acid plane is perpendicular to the reacting C=C bond). In the norbornene and norbornadiene epoxidation all TSs but one prefer the spiro geometry. The *syn,endo*-TS of the norbornadiene reaction adopts a planar-like geometry accompanied by asynchronous C–O bond formation. For the peroxyformic acid epoxidation of *anti*- and *syn*-sesquinornbornene, substrates that for steric reasons cannot easily accommodate a spiro TS, we managed to locate only a planar-like and a planar TS, respectively. These TSs exhibit such a high asynchrony in C–O bond formation that they must be classified as nonconcerted; that is, only one C–O bond of the oxirane ring is appreciably formed at the TS. IRC analysis, downhill from these TSs to the final epoxides, confirms that formation of one of the oxirane C–O bonds takes place first while that of the second one commences afterward, however, in a “one-step” process without formation of any intermediate. Peroxy acid epoxidations via planar TSs can be classified as nonconcerted one-step processes. It should be emphasized that these TSs provide the first examples of planar TSs for C=C epoxidation with peroxy acid located with restricted DFT and post-HF methods.

Theoretical data correctly reproduce the experimental *syn* facial selectivity of norbornene and norbornadiene reactions, and also the theoretically evaluated activation free energies (in the appropriate solvent) compare well with the experimental data for norbornene, norbornadiene, tetramethylethene, and *anti*- and *syn*-sesquinornbornene reactions. Free energy activation data demonstrate that planar TSs can be achieved without a considerable energy expense with respect to spiro TSs.

**Acknowledgment.** Support of this work by MURST (National Project Attivazione di Specie Perossidiche in Processi innovativi di Ossidazione selettiva) (Rome Italy) is gratefully acknowledged. We also thank CIC-AIA (University of Modena) for use of their computer facilities.

**Supporting Information Available:** Cartesian coordinates of all B3LYP/6-311+G(d,p) TSs reported and figures and Cartesian coordinates for TS *syn,endo-1* and the spiro-like TS for *anti*-sesquinornbornene epoxidation located at the B3LYP/6-31G(d) level. This material is available free of charge via the Internet at <http://pubs.acs.org>.

JO026141W